EPIGENETICS
2022, VOL. 17, NO. 12, 1786–1799
https://doi.org/10.1080/15592294.2022.2080995

Taylor & Francis
Taylor & Francis Group

RESEARCH PAPER

ZNF582 promoter methylation predicts cervical cancer radiosensitivity and ZNF582 protein overexpression reduces radiosensitivity by cell cycle arrest in S phase

Nayiyuan Wu[a,#], Xiaoyun Zhang[a,b,#], Miaochen Zhu[a,c,#], Chao Fang[a], Xiaoting Liu[d], Ying Wang[a], He Li[a], Siye Liu[a], Hong Ting[a], Chongzhen Qin[e], Qianjin Liao[a], JingTing Cai[a], and Jing Wang[a]

[a]Hunan Cancer Hospital, The Affiliated Cancer Hospital of Xiangya School of Medicine, Central South University, Changsha, Hunan, China; [b]The second people's hospital of Yueyang City, Hunan, China; [c]Graduate Collaborative Training Base of Hunan Cancer Hospital, University of South China, Hengyang, Hunan, China; [d]The second people's hospital of human province, Changsha, China; [e]Department of Pharmacy, the First Affiliated Hospital of Zhengzhou University, Zhengzhou, Henan, China

ABSTRACT

This study aimed to investigate the relationship between *ZNF582* promoter methylation (*ZNF582*^{m}) level and radiosensitivity of cervical cancer and its biological basis. This was a prospective multi-center clinical study, comprising two independent cohorts of locally advanced cervical cancer patients. Exfoliated cervical cells were collected at 0, 24, 30, 36, 48, and 64 Gy to test *ZNF582*^{m} levels. Radiotherapy response was evaluated according to RECIST Version. RT-PCR and WT were used to detect the mRNA and protein expression levels; MTT and flow cytometry were used to detect the cell viability and cell cycle, respectively. While clone formation and subcutaneous tumorigenesis in nude mice were used to detect the growth of HeLa cells with/without *ZNF582* overexpression. In the first cohort, 22 cases achieved complete remission (CR) or partial response (PR), and the other 28 cases exhibited stable disease (SD). Radiotherapy reduced *ZNF582*^{m} levels among all patients. Initial lever of *ZNF582*^{m} was significantly higher in the Responder (CR + PR) group than in the SD group. Also, patients with higher initial lever *ZNF582*^{m} were more sensitive towards radiotherapy than *ZNF582*$^{m\text{-}low}$ patients. The second cohort confirmed the above results. The amplitude of *ZNF582*^{m} levels were related to the radiotherapeutic response; some patients of *ZNF582*$^{m\text{-}low}$ showed a transient increase in *ZNF582*^{m}, and present greater radiosensitivity than other *ZNF582*$^{m\text{-}low}$ patients. In vitro, ZNF582 protein overexpression promoted cell cycle arrest in S phase. These results suggested that higher *ZNF582*^{m} levels predicted greater radiosensitivity in clinical cervical cancer cases. Overexpressed ZNF582 conferred radioresistance by cell cycle arrest in vitro.

ARTICLE HISTORY
Received 23 January 2022
Revised 12 May 2022
Accepted 18 May 2022

KEYWORDS
Cervical cancer; radiosensitivity; ZNF582; methylation; cell cycle

Introduction

Invasive cervical cancer is a leading cause of cancer death in women worldwide [1,2]. More than 85% of new cases and 90% deaths occurred in developing countries [3,4]. A large proportion of new cases in developing countries are already at an advanced stage (IB2 or more) at diagnosis [5,6]. Most advanced cervical cancer cases receive external beam radiotherapy and brachytherapy with or without chemotherapy as standard treatment [6–8]. Radiotherapy has been used as a cancer treatment for more than a century, and with continued progress in precision delivery, the tumour-targeted dose has greatly increased. However, adverse reactions such as radiation vaginitis, cystitis, and proctitis seriously affect the quality of life of patient [9]. These side effects may be exacerbated by radiotherapy resistance, indeed, resistance to radiotherapy accounts for most therapeutic failures in cervical cancer patients [10,11]. These failures highlight the necessity of developing personalized radiotherapy treatments for cervical cancer and identify reliable biomarkers for predicting treatment response.

Zinc Finger Protein 582 (ZNF582) is located on chromosome 19 that encodes a nuclear protein which contains one KRAB-A-B domain and nine zinc-finger motifs. ZNF582 protein is predicted to be an intracellular protein transcription factor, and ZNF582 gene may also be involved in DNA damage response, proliferation, cell cycle control, and

CONTACT Jing Wang wangjing0081@hnca.org.cn; JingTing Cai Caicaijingting@hnca.org.cn; Qianjin Liao Liaomarch-on@126.com Hunan Cancer Hospital, The Affiliated Cancer Hospital of Xiangya School of Medicine, Central South University, 283, Tongzipo Road, Changsha 410013, Hunan, China
[#]Nayiyuan Wu, Xiaoyun Zhang, and Miaochen Zhu contributed equally to this work.

tumour transformation [12,13]. In 2012, *ZNF582* promoter was found to be hypermethylated in cervical cancer tissues for the first time [14]. Our previous studies have shown that *ZNF582* promoter was hypermethylated in cervical cancer [15–19] and *ZNF582* promoter hypermethylated cervical adenocarcinoma patients demonstrated better prognosis [16]. We also found that *ZNF582* promoter methylation levels were reduced in concurrent chemoradiotherapy (CCRT) patients compared with that in non-CCRT patients in cervical adenocarcinoma patients [19]. However, the relationship between *ZNF582* promoter methylation level and chemoradiotherapy sensitivity in cervical cancer and its potential mechanism are still unclear.

Materials and methods

Study design and patients cohort

This was a prospective multicenter study conducted between October 2017 and May 2019. The subject was composed of two cohorts with newly diagnosed invasive cervical cancer. The inclusion criteria were as follows: (1) histologically confirmed cervical cancer, (2) clinical stages IB2-IVA (FIGO 2009), (3) no prior anti-cancer treatment, and (4) available pretreatment computed tomography (CT) scan. Exclusion criteria were as follows: (1) patients with a history of previous chemotherapy or radiotherapy, (2) patients with a diagnosis of other cancers, or (3) patients with distant metastatic disease (para-aortic nodes involvement was not included).

All patients received image-guided external beam radiotherapy (EBRT) and brachytherapy (BT) with a total dose of 85–90 Gy (EQD2, equivalent dose in 2 Gy single-dose fractions). EBRT used 3D conformal technology at a dose of 1.8–2.0 Gy/fraction with a dose range of 45–50 Gy, while BT boost was volumetrically planned and delivered as weekly high-dose-rate fractions of 8 Gy EQD2 each after 15 times of EBRT. If feasible, cisplatin (40 mg/m^2) chemotherapy or carboplatin (AUC = 2) were given simultaneously every week for 4–6 weeks. Cases were divided into the following two stages:

The first stage: cervical exfoliated cells were collected at 0, 24, 30, 36, 48, and 64 Gy, respectively. The cells were centrifuged and stored in phosphate-buffered saline (PBS) at −20°C immediately.

The response to radiotherapy was evaluated by two skilled radiologists based on Response Evaluation Criteria in Solid Tumours (RECIST) Version 1.1 with the following specific standards: 1. complete remission (CR), defined as disappearance of all target foci; 2. partial response (PR), defined as a ≥30% reduction in total lesion diameter from baseline; 3. stable disease (SD), defined as an increase of <20% or a reduction of <30% in total lesion diameter from baseline; 4. progressive disease (PD), defined as a ≥20% increase in total lesion diameter from baseline. ROC curve analysis to determine the best cut-off value of *ZNF582* methylation levels for discerning Responder (CR + PR) group from SD and PD groups.

In the second stage, we confirmed the research result by an independent cohort at three centres (Hunan Cancer Hospital, Shandong Cancer Hospital, and Liaoning Cancer Hospital).

The study protocol was approved by the Institutional Review Board of Hunan Cancer Hospital.

DNA preparation

Genomic DNA (gDNA) was extracted from the collected cells using the QIAamp DNA Mini Kit (Qiagen GmbH, Hilden, Germany). A BioSpec-nano spectrophotometer (Shimadzu Corporation, Tokyo, Japan) was used to quantify the amount of extracted DNA.

ZNF582 promoter methylation tests

DNA was subjected to bisulphite conversion using the EZ DNA Methylation-Gold™ Kit (Zymo Research, CA, USA). The methylation levels of *ZNF582* were determined using the qPCR kit (Hongya Gene Technology Co., Ltd.) and calculated the methylation index (M-index) using the formula: $10{,}000 \times 2^{[(\text{Cp of COL2A}) - (\text{Cp of ZNF582})]}$, the type II collagen gene (COL2A) was designed as the internal reference and tested with each specimen. The crossing point (Cp) value for COL2A, which is also the validity indicator of the test, should not be >35. For each sample, two Cp values were obtained: one from ZNF582 and another from COL2A [16,19].

Establishment of *ZNF852* overexpression cell line

HeLa (CLS Cat# 300,194/p772_HeLa, RRID: CVCL_0030) cells were transfected with 20 μg of *ZNF582* adenoviral vector (Vigene Biosciences, Rockville, MD, USA; NM_144690) or controlled adenoviral vector (Vigene Biosciences, Rockville, MD, USA; pLent-GFP-Puro-CMV). The transferred cells were then selected with puromycin.

Cell viability assay

Cultured cells in the logarithmic growth phase were harvested using trypsin and seeded onto 96-well plates at 5000 cells/well. The culture medium was aspirated off, and 100 μL XTT solution (20-300-1000, Biological Industries) was added at the indicated times, and incubated at 37°C for 3 hours. Optical density values were measured at 450 nm as an estimate of viable cell number using a microplate reader.

Cell cycle analysis by flow cytometry

Cells were collected and washed with cold PBS, fixed in 70% ethanol, and stored at 4°C overnight. The fixed cells were washed with PBS and stained with 500 μL propidium iodide (PI; BD Biosciences, Franklin Lakes, NJ, USA) in dark conditions for 30 minutes. The distribution of cell cycle stages was measured by flow cytometry within 1 hour. Cell debris and fixation artefacts were gated out.

Quantitative RT-PCR (Q-PCR)

Total RNA was extracted from cultured cells using Trizol (Invitrogen, Carlsbad, CA, USA) and reverse transcribed into cDNA using oligo (dT) primers and a cDNA synthesis kit (Invitrogen, USA) according to the manufacturer's protocol. Gene expression was assessed by qRT-PCR using SYBR Premix Dimer Eraser (Perfect Real-Time) assay kits and the following primers:

GAPDH-forward, 5';-GAAGGTGAAGGTCGGAGTC-3';

GAPDH-reverse, 5'-GAAGATGGTGATGGGATTTC-3';

ZNF582-forward 5'-GAGGAGGCGGCAGCTCTACC;

ZNF582-reverse 5'-GAAACGGCAAGACCCAGTGAGAC.

Real-time PCR was performed using the Roche LC480 PCR System, and results were analysed using the comparative Cp method.

Western blotting and immunofluorescence assays

Crude cellular proteins were separated by SDS-PAGE and transferred to nitrocellulose membranes. Membranes were blocked in 5% non-fat milk and probed with primary antibodies against ZNF582 (ABclonal, A14453; 1:500), p21/Waf (Cell Signaling Technology, 9932kit, 1:1000), p27(KIP1) (Cell Signaling Technology, 9932kit, 1:1000), p21 (Cell Signaling Technology, 9932kit, 1:1000), CyclinD1 (Cell Signaling Technology, 9932kit, 1:1000), CDK2 (Cell Signaling Technology, 9932kit, 1:1000), CDK4 (Cell Signaling Technology, 9932kit, 1:1000), PI3K (Abcam, ab191606; 1:1000), Akt (Cell Signaling Technology, 9272, 1:1000), and α-tubulin (Abcam, ab7291, 1:5000) overnight at 4°C. Membranes were incubated with secondary antibodies for 1.5 hours and detected using a Bio-Rad imaging system.

Animal experiments

Female BALB/c nude mice (RRID:IMSR_ORNL:BALB/cRl) at 6 weeks of age were obtained from SLA Laboratory Animal (Changsha, China) and housed in a specific pathogen-free facility. Individual mice was subcutaneously injected with 5×10^6 HeLa cells. Four weeks after the inoculation, the mice were sacrificed and the tumours dissected out. The experimental protocol was approved by the Animal Care Committee of Hunan Cancer Hospital.

Statistical analysis

Statistical analyses were performed using SPSS (RRID: SCR_002865)18.0. Continuous variables are presented as mean ± standard deviation. Qualitative variables are described by frequencies and percentages. The comparison between groups was conducted by *t*-test, ANOVA, Chi-squared test, or non-parametric test (Mann–Whitney Test) (selected according to the data type) and a *P*-value of <0.05 was considered to indicate significance.

Results

Radiotherapy reduced *ZNF582* promoter methylation levels

The first cohort included 50 patients with locally advanced cervical cancer who received concurrent chemoradiotherapy (CCRT) (n = 37) or radiotherapy alone (n = 13) (Figure 1). The patients' characteristics are summarized in Table 1. Cervical exfoliated cells were collected at 0, 24, 30, 36, 48, and 64 Gy doses (Figure 2a). All patients revealed a significant decline in *ZNF582* promoter methylation levels ($ZNF582^{m}$) during radiotherapy (Figure 2b). The tendency of $ZNF582^{m}$ levels during radiotherapy was consistent with squamous cell carcinoma antigen (SCC-Ag) (Figure 2c).

Higher $ZNF582^{m}$ predicted greater radiosensitivity

In the first group, 22 cases achieved a CR or PR (Responder group), whereas 28 exhibited SD (Figure 1); $ZNF582^{m}$ was significantly higher in the Responder group than in the SD group, both in patients receiving radiotherapy only or chemoradiotherapy (Figure 3a, b, c). In ROC curve, a cut-off value of 1182 stratified Responder patients and SD patients with area under the curve (AUC) of 81.01%, sensitivity of 82.14%, and specificity of 72.73% (Figure 3d).

Among the 50 patients, 21 were defined as high-level *ZNF582* methylation ($ZNF582^{m\text{-}high}$) cases, while 29 defined as low-level ZNF582 methylation

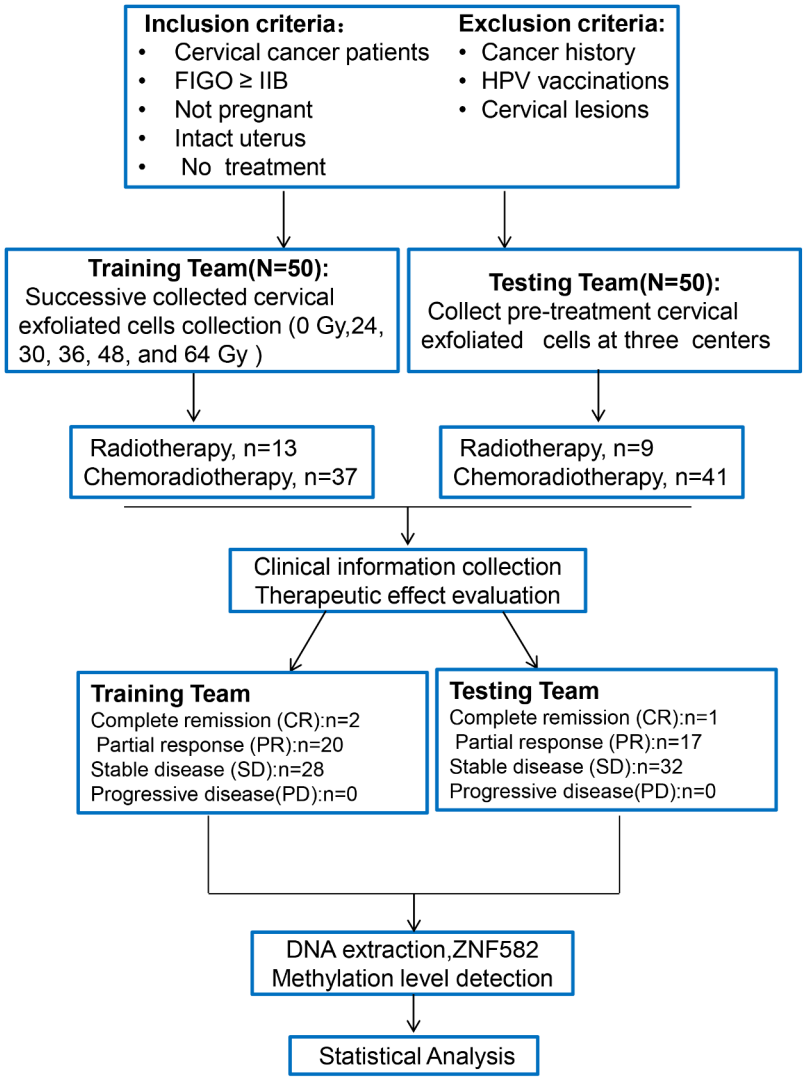

Figure 1. Study design and patient cohort for this study.
FIGO, Federation of Gynaecology and Obstetrics.

Table 1. Characteristics of *ZNF582*$^{m\text{-}High}$ and *ZNF582*$^{m\text{-}Low}$ subjects in the first cohort.

Characteristics	Patients (n = 50)	*ZNF582*$^{m\text{-}High}$ (n = 21)	*ZNF582*$^{m\text{-}Low}$ (n = 29)	*P* value
Specimen				
Squamous cell carcinoma	46	20	26	0.651
Adenocarcinoma	1	0	1	
Adenosquamous carcinoma	3	1	2	
Age (years)				
<50	9	5	4	0.363
≥50	41	16	25	
FIGO stage				
<IIB	0	0	0	1.000
≥IIB	50	21	29	
Differentiation				
Well/moderate	33	15	18	0.288
Poorly	11	3	8	
Unknown	6	3	3	
CCRT				
With	37	14	23	0.314
Without	13	7	6	
LNM				
Yes	34	13	21	0.432
No	16	8	8	

FIGO, International Federation of Gynaecology and Obstetrics; CCRT, concurrent chemoradiotherapy; LNM, Lymph node metastasis.

(*ZNF582*$^{m\text{-}low}$) case according to ROC curve (Figure 3d). The *ZNF582*$^{m\text{-}high}$ patients were more sensitive to radiotherapy than *ZNF582*$^{m\text{-}low}$ patients, both in the entire cohort (76.2% vs. 20.7%) and in patients receiving radiotherapy only (85.7% vs. 0%) (Table 2). Representative computed tomography (CT) images are shown in Figure 3e.

The above results were confirmed by an independent cohort; *ZNF582*^{m} was significantly higher in the Responder group than in the SD group, not only in the entire cohort (n = 50, Figure 4a) but also in the patients receiving radiotherapy only (n = 9, Figure 4b) or chemoradiotherapy (n = 41, Figure 4c). ROC curve acquired 84.38% sensitivity and 83.33% specificity (Figure 4d). The *ZNF582*$^{m\text{-}high}$ patients were more sensitive to radiotherapy than the *ZNF582*$^{m\text{-}low}$ patients (Table 3). The characteristics of the first cohort and second cohort are presented in Table 4

A transient increase of ZNF582^{m} *levels during radiotherapy predicted greater radiosensitivity in the ZNF582*$^{m\text{-}low}$ *cases*

A subset of patients (5 of 29 cases) in *ZNF582*$^{m\text{-}low}$ group showed a transient increase of *ZNF582*^{m} levels after receiving 24 Gy radiotherapy, representative cases are shown in Figure 5a. This suggested that radiation could increase *ZNF582*^{m} levels and synergistically enhance the radiosensitivity. In the *ZNF582*$^{m\text{-}high}$ levels group, *ZNF582*^{m} levels decreased rapidly in some cases (12 of 21 cases), while decreased slowly in others (Figure 5b). There was no significant difference in radiosensitivity between these two subgroups.

ZNF582 protein overexpression induced cell cycle arrest and radioresistance in HeLa cells

Our previous study demonstrated that *ZNF582*^{m}-negative status was correlated with high ZNF582 protein expression, and *ZNF582* overexpression increased the radiation and chemotherapy resistance of cervical cancer cells [16]. To investigate the underlying mechanisms, we transfected *ZNF582* into HeLa cells (Figure 6a, b). ZNF582 protein overexpressing significantly reduced cell proliferation (Figure 6c), colony formation (Figure 6d) and tumour growth (Figure 6e) of HeLa cell. Transcriptome sequencing showed that cell cycle-related pathways were significantly up-regulated in HeLa cells after ZNF582 protein overexpression (Figure 6f). The flow cytometry showed that the proportion of S phase was significantly increased and G1 phase decreased in the *ZNF582* overexpressing HeLa cells (Figure 6h), suggesting that *ZNF582* overexpression arrested the cell cycle in the S phase. Further, *ZNF582* overexpressing HeLa cells demonstrated resistance to

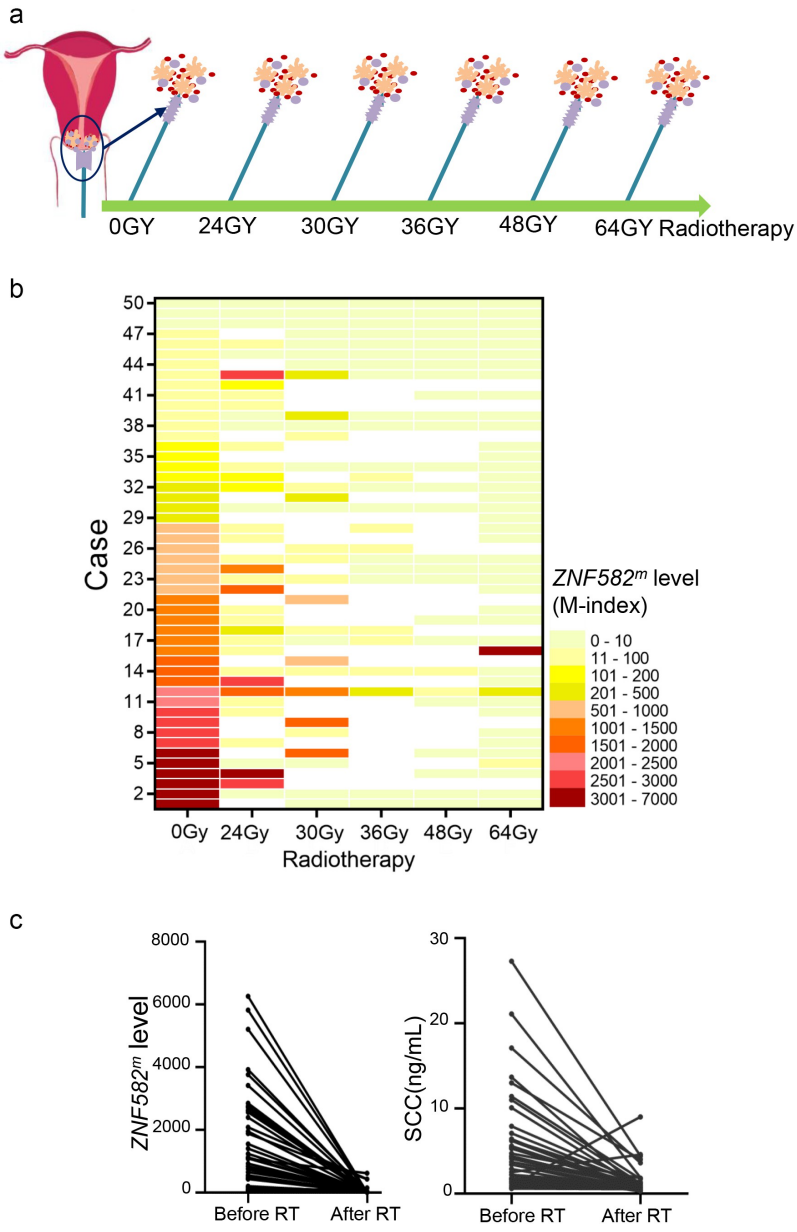

Figure 2. Changes in *ZNF582* methylation level (*ZNF582*^{m}) during radiotherapy.

a. Flow chart of specimen collection. Exfoliated cervical cancer cells were collected at 0, 24, 30, 36, 48, and 64 Gy. **b**. Heat map of *ZNF582*^{m} during radiotherapy (darker colour indicates higher *ZNF582*^{m}). Each row represents one case. c. Both *ZNF58*^{m} and SCC decreased significantly during radiotherapy.

radiotherapy compared to control cells (Figure 6f). Western blotting revealed that *ZNF582* overexpressing enhanced p27(KIP1), p21, CDK2, and CDK4 expression, and attenuated PI3K and Akt expression in HeLa cells (Figure 6g); and immunohistochemical analysis of mice tumour tissues confirmed these phenomena (Figure 6h), suggesting ZNF582 protein overexpression may induce S phase arrest by stimulating p27(KIP1)/p21/CDK2/4 signalling in HeLa cells. Cell cycle stage is associated with radiation sensitivity, with the highest sensitivity in G2/M phase and the lowest in S phase [20–24]. Overexpressed ZNF582 may reduce cervical cancer radiosensitivity by arresting the cell cycle in S phase.

Discussion

Cervical cancer is one of the most common gynaecological malignancies in the world. It is estimated that

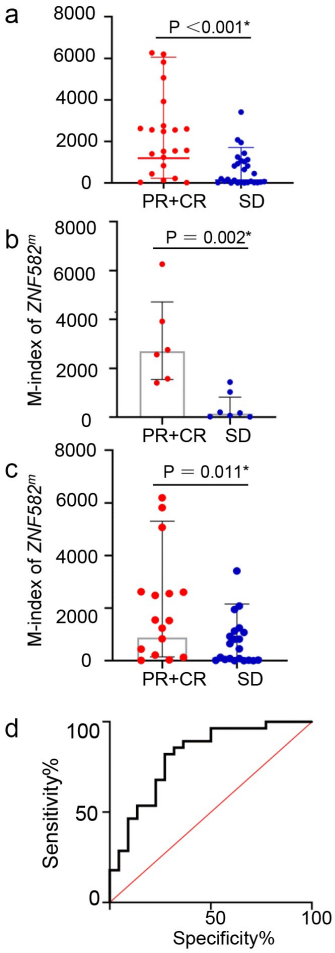

	ZNF582^{m} of Total	
	PR+CR	SD
Case	22	28
Mean±SD	2356±1985	641±825
P-value	<0.001*	

	ZNF582^{m} of only Radiotherapy	
	PR+CR	SD
Case	6	7
Mean±SD	3080±1805	422±571
P-value	0.002*	

	ZNF582^{m} of chemoradiotherapy	
	PR+CR	SD
Case	16	21
Mean±SD	2084±509	714±893
P-value	0.011*	

	ZNF582^{m}
Cutoff-value	1182
Sensitivity	82.14 %
Specificity	72.73%
AUC	81.01 %
P-value	0.0002**

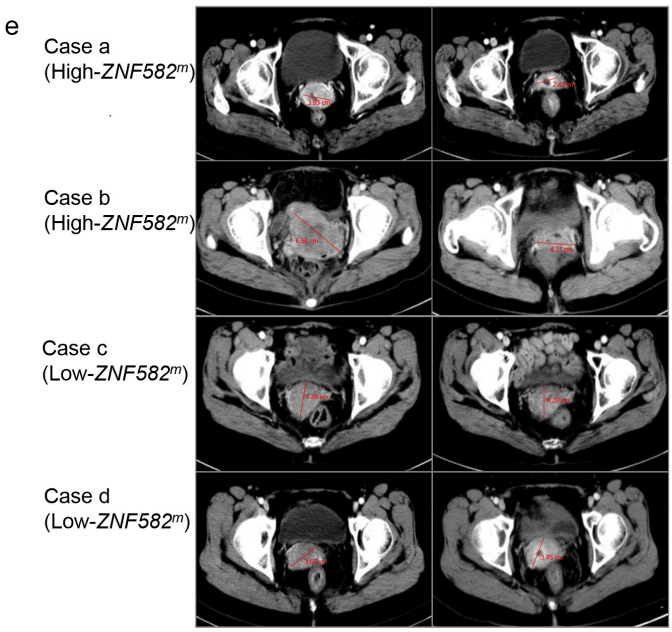

Figure 3. Patients with higher initial lever of *ZNF582*^{m} were more sensitive towards radiotherapy than *ZNF582*$^{m\text{-}low}$ patients. **a**. Among 50 patients, average initial lever of *ZNF582*^{m} (M-index) was significantly greater in the CR + PR group than in the SD group [2356 ± 1985 vs. 641 ± 825, $P < 0.05$* by non-parametric test (Mann–Whitney Test)]. **b, c**. Average *ZNF582*^{m} values were also higher in the CR + PR group than in the SD group in both chemoradiotherapy cases (b) and radiotherapy-only cases (c). **d**. Receiver operating characteristic (ROC) analysis for stratifying CR + PR group from SD group by *ZNF582*^{m}. The calculated cut-off M-index value of 1182 distinguished CR+ PR from SD with 82.14% sensitivity and 72.73% specificity. The AUC was 81.01%. **e**. Representative CT/MR images from *ZNF582* $^{m\text{-}high}$ and *ZNF582* $^{m\text{-}low}$ patients before and after radiotherapy.

Table 2. Comparison of the efficacy of radiotherapy in the first cohort with *ZNF582*$^{m\text{-}High}$ or *ZNF582*$^{m\text{-}Low}$.

	Cases	CR+PR	SD	ORR(%)
Total				
ZNF582$^{m\text{-}High}$	21	16	5	76.2
ZNF582$^{m\text{-}Low}$	29	6	23	20.7
P-value		<0.001*		
Radiotherapy Alone				
ZNF582$^{m\text{-}High}$	7	6	1	85.7
ZNF582$^{m\text{-}Low}$	6	0	6	0
P-value		0.005*		
Chemoradiotherapy				
ZNF582$^{m\text{-}High}$	14	10	4	71.4
ZNF582$^{m\text{-}Low}$	23	6	17	26.1
P-value		0.015*		

ORR: Objective Remission Rate

94 million cases will increase in low- and middle-income countries requiring external beam radiotherapy from 2015 to 2035, of which 70 million will also require treatment with brachytherapy [25]. Chemoradiotherapy (CRT) is the standard treatment for locally advanced cervical cancer [4], and radiotherapy provides the greatest survival benefit for cervical cancer patients. However, neither radiotherapy nor chemotherapy is effective for a substantial proportion of cases, and the 5-year survival rate remains at only 40–50% [26].One possible explanation for these unsatisfactory results is the radioresistance at baseline. Therefore,continued efforts are required to improve CRT and identify biomarkers for patients at risk of poor therapeutic response.

Our previous studies have shown that *ZNF582*^{m}-positive cervical cancer patients have a better prognosis, but the underlying mechanisms are undefined. Chemoradiotherapy resistance is associated with poor prognosis of cervical cancer, especially in advanced cases, suggesting that *ZNF582*^{m} status may regulate chemo- and/or radiosensitivity. In this study, we confirmed that patients with high levels of *ZNF582* promoter methylation were more sensitive to radiation therapy (Figures 3, 4 and Tables 2, 3). SCC-Ag is most commonly used to monitor the therapeutic effect, recurrence, metastasis, and prognosis of cervical cancer [8,27–29]. Similar to SCC, *ZNF582*^{m} was significantly reduced after radiotherapy (Figure 2c).

Another major finding of this study was that radiation therapy could induce an initial transient increase in *ZNF582*$^{-low}$ group, and these patients presented greater sensitivity compared to other hypomethylated patients. Further studies are needed to explore predictors and the mechanisms underlying this unusual response to expand the clinical application of radiotherapy.

We also explored the underlying mechanisms of *ZNF582*^{m} levels and radiotherapy sensitivity of cervical cancer. Methylation is a negative regulator of gene expression. We reported in our previous study that *ZNF582* promoter hypermethylation correlated with low ZNF582 protein expression, and similarly, low *ZNF582*^{m} levels correlated with high protein expression [16]. The expression levels of ZNF582 were extremely low in HeLa cells (Figure 6a, b). ZNF582 protein overexpression delayed S/G2-phase in HeLa cells, inducing p27/p21 accumulation and inhibition of the PI3K/Akt pathway, and ZNF582 protein overexpression increased resistance to radiation (Figure 6). Tumour cells in different cell cycle stages showed different sensitivity to radiation, with the highest sensitivity in G2/M phase and the lowest in S phase [21–23]. Accumulation of p27 [30–35], p21 [36–38], CDK2 [39], and CDK4 [40] and inhibition of PI3K/Akt/CyclinD1 [41] may contribute to S/G2 cell cycle arrest. Our data suggested that ZNF582 protein overexpression delayed S/G2-phase in HeLa cells and increased resistance to radiation. These findings may explain why *ZNF582*$^{m\text{-}low}$ patients were resistant to radiotherapy and conferred poorer prognosis [16].

This study demonstrated that *ZNF58*^{m} levels in exfoliated cervical cells are a reliable biomarker for predicting the response to radiotherapy and monitoring therapeutic efficacy. As a biomarker,

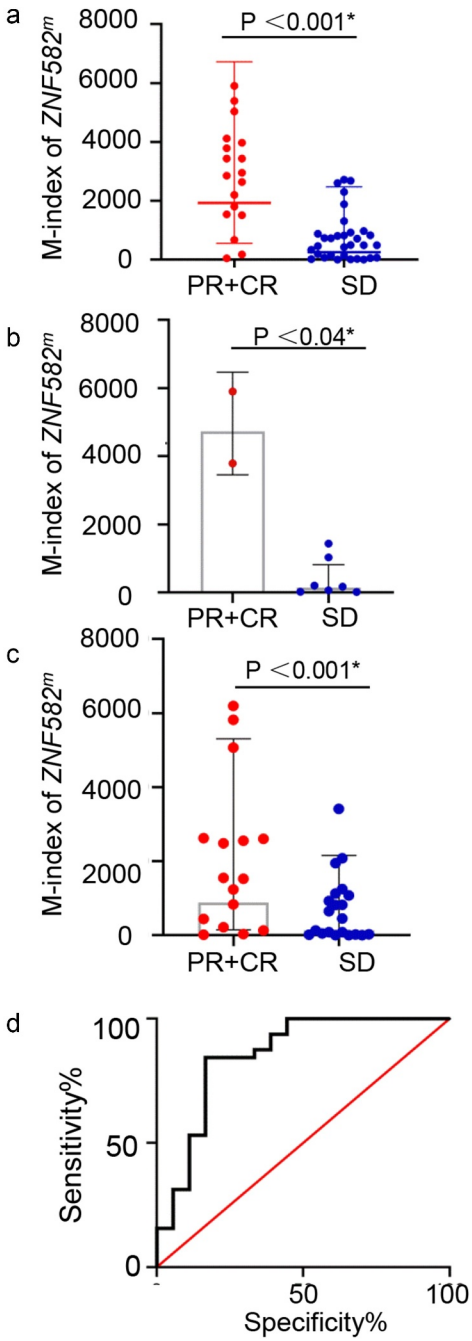

	ZNF582m of Total	
	PR+CR	SD
Case	18	32
Mean±SD	2761±1712	761±821
P-value	<0.001*	

	ZNF582m of only Radiotherapy	
	PR+CR	SD
Case	2	7
Mean±SD	4847±1496	504±421
P-value	0.04*	

	ZNF582m of chemoradiotherapy	
	PR+CR	SD
Case	16	25
Mean±SD	2613±1607	833±895
P-value	<0.001*	

	ZNF582m
Cutoff-value	1182
Sensitivity	84.38%
Specificity	83.33%
AUC	85.24%
P-value	<0.0001

Figure 4. An independent cohort confirmed the patients with *ZNF582*^{m} higher initial lever achieving better response than low baseline *ZNF582*^{m} patients.

a. Among 50 patients, average initial lever of *ZNF582*^{m} (M-index) was significantly greater in the CR + PR group than in the SD group [4847 ± 1496 vs. 504 ± 421, $P < 0.05$* by non-parametric test (Mann–Whitney Test)]. **b,c**. Average ZNF582^{m} values were also higher in the CR + PR group than in the SD group in both chemoradiotherapy cases (b) and radiotherapy-only cases (c). **d**. Receiver operating characteristic (ROC) analysis for stratifying CR+ PR patients from SD patients by *ZNF582*^{m}. The calculated cut-off M-index value of 1182 distinguished CR + PR from SD with 84.38% sensitivity and 83.33% specificity. The AUC was 85.24%.

ZNF582^{m} has several advantages: (1) it could be measured in non-invasively exfoliated cells; (2) it provides not only a pre-treatment predictor of response but also allows therapeutic monitoring during the course of treatment; and (3) it could be accurately and inexpensively detected with conventional reagents. We concluded that *ZNF58*^{m} measurement is helpful for early screening,

Table 3. Comparison of the efficacy of radiotherapy in the second cohort with *ZNF582*$^{m\text{-}High}$ or *ZNF582*$^{m\text{-}Low}$.

	Cases	CR+PR	SD	ORR(%)
Total				
ZNF582$^{m\text{-}High}$	21	15	6	71.43
ZNF582$^{m\text{-}Low}$	29	3	26	10.34
P-value		<0.001*		
Radiotherapy Alone				
ZNF582$^{m\text{-}High}$	2	2	0	100
ZNF582$^{m\text{-}Low}$	7	0	7	0
P-value		0.028*		
Chemoradiotherapy				
ZNF582$^{m\text{-}High}$	19	13	6	68.42
ZNF582$^{m\text{-}Low}$	22	3	19	13.64
P-value		<0.001*		

ORR: Objective Remission Rate

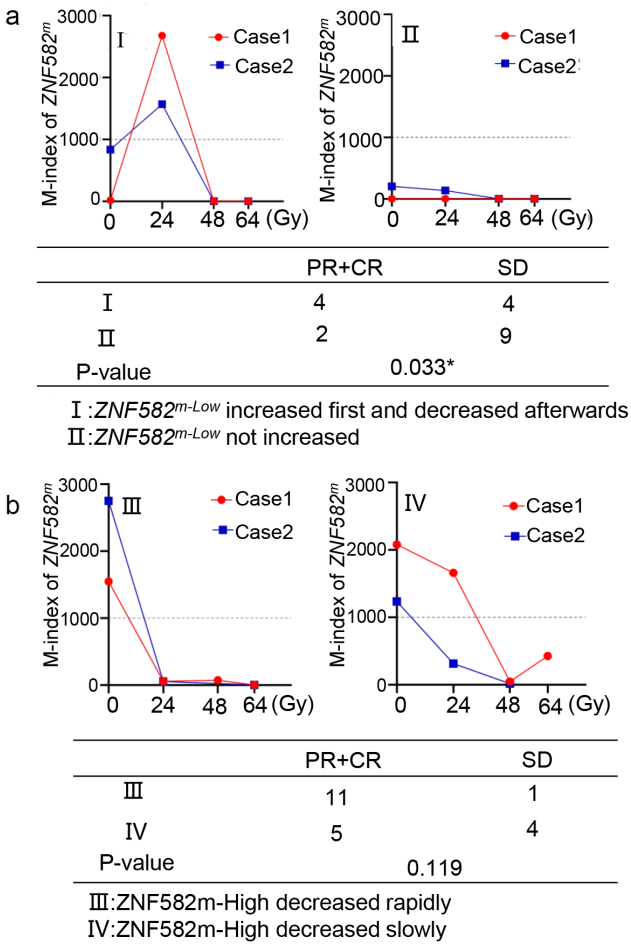

Figure 5. The amplitude of *ZNF582*^{m} levels were related to radiotherapeutic response.

a. I) Representative *ZNF582*$^{m-low}$ cases showing a transient increase in *ZNF582*^{m} after receiving 24 Gy and then a rapid decline; II) Representative *ZNF582*$^{m-low}$ cases showing a progressive decline throughout the course of radiotherapy; **b**. III) Representative *ZNF582*$^{m-high}$ cases showing a rapid decline after 24 Gy; IV) Representative *ZNF58* $^{m-high}$ cases showing a gradual decline during radiotherapy.

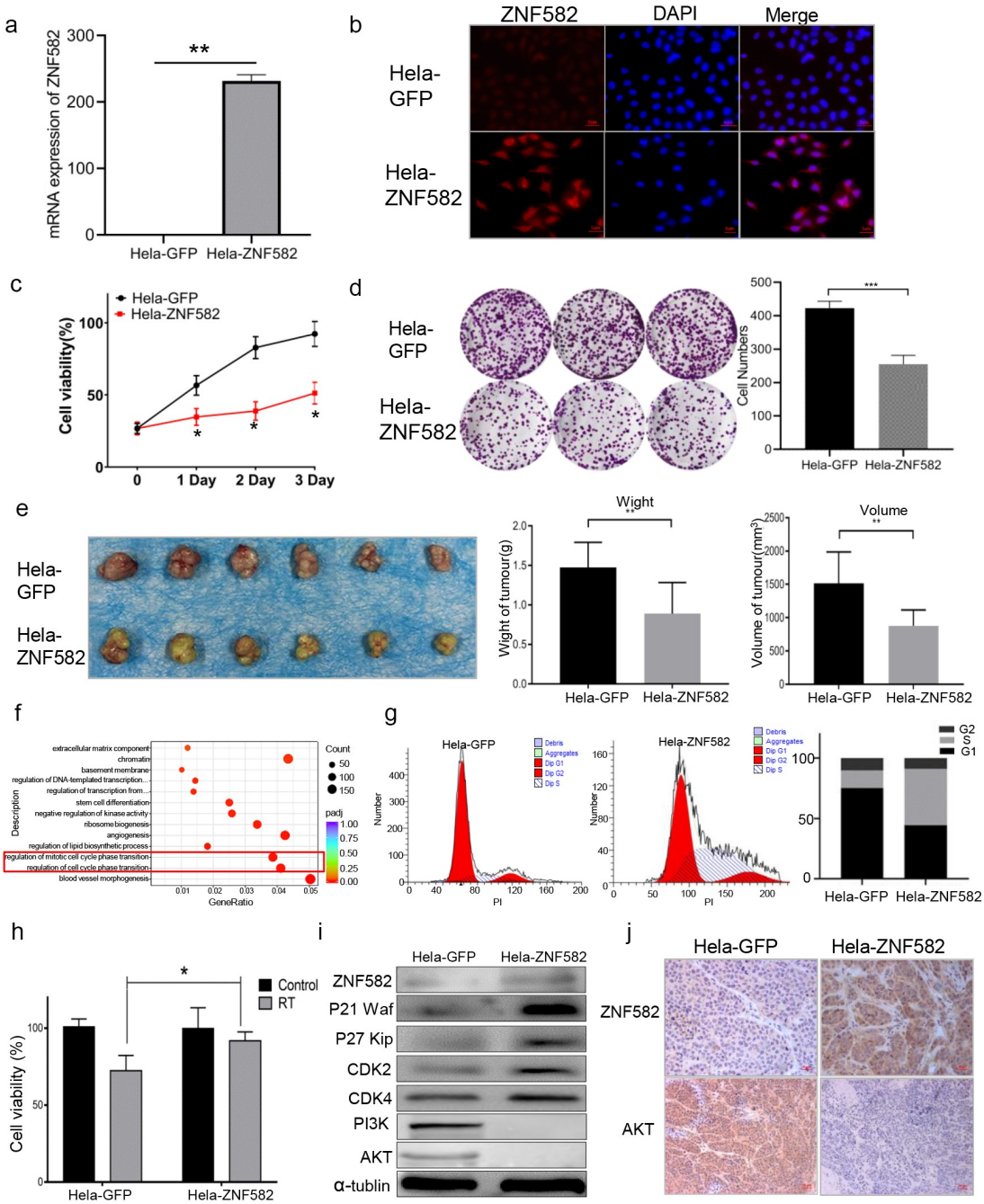

Figure 6. ZNF582 overexpression induced S phase arrest in Hela cells.

a,b. Q-PCR and immunocytochemical tested the expression of ZNF582 mRNA and protein in HeLa cells transfected with vector control (GFP) or ZNF582 vector. **c**. Cell proliferation rate of Hela-ZNF582 and Hela-GFP. **d**. Colony formation ability significantly decreased in the HeLa cells with ZNF582 overexpression. **e**. In the xenografts of HeLa cells in nude mice, the tumour volume and weight of the ZNF582-overexpressing cells were significantly lower than those in the control group. **f**. Bubble chart. GO enrichment analysis of differentially expressed genes of Hela-ZNF582 compare with Hela-GFP. **g**. Cell cycle stage was detected by flow cytometry. **h**. Viabilities of HeLa cells transfected with ZNF582 or GFP (control) after 6 Gy radiation treatment (RT) for 48 h. **i**. Cell cycle-associated molecules by HeLa-GFP and HeLa-ZNF582 cells determined by western blotting. **j**. ZNF582 and Akt expression in the tumour tissues were determined by immunohistochemistry. Data are expressed as mean ± SD of three separate experiments per group (magnification ×400; scale bars 20 μm; $^{*}P < 0.05$, $^{**}P < 0.01$, $^{***}P < 0.001$ vs. the controls by *t*-test).

Table 4. Characteristics of first cohort and second cohort subjects.

Characteristics	Patients (n = 50)	First cohort (n = 50)	Second cohort (n = 50)	*P* value
Specimen				
Squamous cell carcinoma	92	46	46	
Adenocarcinoma	3	1	2	0.766
Adenosquamous carcinoma	5	3	2	
Age (years)				
<50	13	9	4	0.147
≥50	87	41	46	
FIGO stage				
<IIB	2	0	2	0.475
≥IIB	98	50	48	
Differentiation				
Well/moderate	57	33	24	0.320
Poorly	24	11	13	
Unknown	19	6	13	
CCRT				
With	78	37	41	0.334
Without	22	13	9	
LNM				
Yes	59	34	25	0.067
No	41	16	25	

FIGO, International Federation of Gynecology and Obstetrics; CCRT, neoadjuvant radio (chemo-) therapy; LNM, Lymph node metastasis.

diagnosis, prediction of radiotherapy response, and prognosis of cervical cancer.

Acknowledgments

The authors thank all the members of Jing Wang laboratory, Hunan Hongya Gene Technology Co., Ltd., and Enago (www.enago.cn) for the English embellishment.

Disclosure statement

No potential conflict of interest was reported by the author(s).

Abbreviations

ZNF582, zinc finger protein 582;*ZNF582*^{m}, methylated ZNF582 gene; RECIST, Response Evaluation Criteria in Solid Tumours; ROC, receiver operating characteristic; CCRT, concurrent chemoradiotherapy; PBS, phosphate-buffered saline; CR, complete remission; PR, partial response; PD, Progressive disease; SD, Stable disease; M-index, the methylation index; HPV, human papillomavirus; gDNA, genomic DNA; QMSP, quantitative methylation-specific PCR; COL2A, The type II collagen gene; Cp, The crossing point; SR, Satisfied response; MR, Modest response; AUC, area under the curve; CT, computed tomography; SCC-Ag, Squamous cell carcinoma antigen; CRT, Chemoradiotherapy; FIGO, Federation of Gynecology and Obstetrics; RT, radiation treatment; SCC, Squamous cell carcinoma; SD, standard deviation; ORR, objective remission rate.

Authors' contributions

XYZ, MCZ, JTC, TH, XTL, and CZQ contributed to sample collection. NYW contributed to the writing of this manuscript. XYZ, NYW, and MCZ contributed to the clinical data evaluation and the molecular experiments. JTC, JW, NYW, and QJL contributed to the conception, design, and final approval of the submitted version. JW and NYW provide financial support. XYZ, YW, CF, SYL, and HL contributed to the technical support for the data analysis. All authors read and approved the final manuscript.

Ethics approval and consent to participate

The study protocol was approved by the Institutional Review Board of Hunan Cancer Hospital and the Animal Ethics Committee of Hunan Cancer Hospital. Informed consent was obtained from all participants in accordance with the Declaration of Helsinki.

Consent for publication availability of data and material

The data that support the findings of this study are available on request from the corresponding author. The data are not publicly available due to privacy or ethical restrictions.

Financial support

This work was supported by the Department of Science and Technology of Hunan Province (2018SK2121, 2020SK2120,

2020JJ5338 and 2021RC2104), the National Natural Science Foundation of China (82,003,050), the Foundation of Social Development Science and Technology Division (kq2004138), and Scientific Research Project of Hunan Health Commission (C2019066).

Authors' information

1. Hunan Cancer Hospital, the Affiliated Cancer Hospital of Xiangya School of Medicine, Central South University, Changsha, Hunan, China. 2. University of South China, Hengyang, Hunan, China. 3. The Second People's Hospital of Yueyang City, Hunan, China. 4. The Second People's Hospital of Hunan Province. 5. Department of Pharmacy, the First Affiliated Hospital of Zhengzhou University, Zhengzhou, China.

Funding

This work was supported Department of science and technology of Hunan Province (2018SK2121, 2020SK2120, 2020JJ5338, 2021RC2104), National Natural Science Foundation of China (82003050).

References

[1] Siegel RL, Miller KD, Jemal A. Cancer statistics, 2019. CA Cancer J Clin. 2019;69(1):7–34.
[2] Miller KD, Nogueira L, Mariotto AB, et al. Cancer treatment and survivorship statistics, 2019. CA Cancer J Clin. 2019;69(5):363–385.
[3] Bray F, Ferlay J, Soerjomataram I, et al. Global cancer statistics 2018: GLOBOCAN estimates of incidence and mortality worldwide for 36 cancers in 185 countries. CA Cancer J Clin. 2018;68(6):394–424.
[4] Bermudez A, Bhatla N, Leung E. Cancer of the cervix uteri. Int J Gynaecol Obstet. 2015;131(2):S88–95.
[5] Wang SM, Qiao YL. Implementation of cervical cancer screening and prevention in China–challenges and reality. Jpn J Clin Oncol. 2015;45(1):7–11.
[6] Kokka F, Bryant A, Brockbank E, et al. Hysterectomy with radiotherapy or chemotherapy or both for women with locally advanced cervical cancer. Cochrane Database Syst Rev. 2015; (4):Cd010260. DOI:10.1002/14651858.CD010260.pub2.
[7] Yang J, Cai H, Xiao Z-X, et al. Effect of radiotherapy on the survival of cervical cancer patients: an analysis based on SEER database. Medicine (Baltimore). 2019;98(30):e16421.
[8] Fu J, Wang W, Wang Y, et al. The role of squamous cell carcinoma antigen (SCC Ag) in outcome prediction after concurrent chemoradiotherapy and treatment decisions for patients with cervical cancer. Radiat Oncol. 2019;14(1):146.
[9] Sabulei C, Maree JE. An exploration into the quality of life of women treated for cervical cancer. Curationis. 2019;42(1):e1–e9.
[10] Li Q, Zhang Y, Jiang Q. SETD3 reduces KLC4 expression to improve the sensitization of cervical cancer cell to radiotherapy. Biochem Biophys Res Commun. 2019;516(3):619–625.
[11] Huang C, Lu H, Li J, et al. SOX2 regulates radioresistance in cervical cancer via the hedgehog signaling pathway. Gynecol Oncol. 2018;151(3):533–541.
[12] Figueroa ME, Lugthart S, Li Y, et al. DNA methylation signatures identify biologically distinct subtypes in acute myeloid leukemia. Cancer Cell. 2010;17(1):13–27.
[13] Huntley S, Baggott DM, Hamilton AT, et al. A comprehensive catalog of human KRAB-associated zinc finger genes: insights into the evolutionary history of a large family of transcriptional repressors. Genome Res. 2006;16(5):669–677.
[14] Huang RL, Chang -C-C, Su P-H, et al. Methylomic analysis identifies frequent DNA methylation of zinc finger protein 582 (ZNF582) in cervical neoplasms. PLoS One. 2012;7(7):e41060.
[15] Liou YL, Zhang T-L, Yan T, et al. Combined clinical and genetic testing algorithm for cervical cancer diagnosis. Clin Epigenetics. 2016;8(1):66.
[16] Wu N-Y-Y, Zhang X, Chu T, et al. High methylation of ZNF582 in cervical adenocarcinoma affects radiosensitivity and prognosis. Ann Transl Med. 2019;7(14):328.
[17] Lin H, Chen T-C, Chang T-C, et al. Methylated ZNF582 gene as a marker for triage of women with Pap smear reporting low-grade squamous intraepithelial lesions - a Taiwanese Gynecologic Oncology Group (TGOG) study. Gynecol Oncol. 2014;135(1):64–68.
[18] Tian Y, Wu NYY, Liou YL, et al. Utility of gene methylation analysis, cytological examination, and HPV-16/18 genotyping in triage of high-risk human papilloma virus-positive women. US: Oncotarget; 2017.
[19] Liou YL, Zhang Y, Liu Y, et al. Comparison of HPV genotyping and methylated ZNF582 as triage for women with equivocal liquid-based cytology results. Clin Epigenetics. 2015;7(1):50.
[20] Sinclair WK, Morton RA. X-ray sensitivity during the cell generation cycle of cultured Chinese hamster cells. Radiat Res. 1966;29(3):450–474.
[21] Sinclair WK, Morton RA. Variations in X-ray response during the division cycle of partially synchronized Chinese hamster cells in culture. UK: Nature. 1963; 199: 1158–1160.
[22] Terasima T, Tolmach LJ. Variations in several responses of HeLa cells to x-irradiation during the division cycle. Biophys J. 1963;3(1):11–33.
[23] Terasima T, Tolmach LJ. X-ray sensitivity and DNA synthesis in synchronous populations of HeLa cells. Science. 1963;140(3566):490–492.

[24] Carlson JG. X-ray-induced prophase delay and reversion of selected cells in certain avian and mammalian tissues in culture. Radiat Res. 1969;37(1):15–30.
[25] Rodin D, Burger EA, Atun R, et al. Scale-up of radiotherapy for cervical cancer in the era of human papillomavirus vaccination in low-income and middle-income countries: a model-based analysis of need and economic impact. Lancet Oncol. 2019;20(7):915–923.
[26] Wright JD, Chen L, Tergas AI, et al. Population-level trends in relative survival for cervical cancer. Am J Obstet Gynecol. 2015;213(5):670.e1–7.
[27] Salvatici M, Achilarre MT, Sandri MT, et al. Squamous cell carcinoma antigen (SCC-Ag) during follow-up of cervical cancer patients: role in the early diagnosis of recurrence. Gynecol Oncol. 2016;142(1):115–119.
[28] Wen YF, Cheng -T-T, Chen X-L, et al. Elevated circulating tumor cells and squamous cell carcinoma antigen levels predict poor survival for patients with locally advanced cervical cancer treated with radiotherapy. PLoS One. 2018;13(10):e0204334.
[29] Shen Q, Lin W, Luo H, et al. Differential expression of aquaporins in cervical precursor lesions and invasive cervical cancer. Reprod Sci. 2016;23(11):1551–1558.
[30] Liu Z, Li J, Chen J, et al. MCM family in HCC: MCM6 indicates adverse tumor features and poor outcomes and promotes S/G2 cell cycle progression. BMC Cancer. 2018;18(1):200.
[31] Wang A, Zeng R, Huang H. Retinoic acid and sodium butyrate as cell cycle regulators in the treatment of oral squamous carcinoma cells. Oncol Res. 2008;17(4):175–182.
[32] Lin CB, Lin CC, Tsay GJ. 6-gingerol inhibits growth of colon cancer cell LoVo via induction of G2/M arrest. Evid Based Complement Alternat Med. 2012;2012:326096.
[33] Sun XL, Zhang X-W, Zhai H-J, et al. Magnoflorine inhibits human gastric cancer progression by inducing autophagy, apoptosis and cell cycle arrest by JNK activation regulated by ROS. Biomed Pharmacother. 2020;125:109118.
[34] Auld CA, Fernandes KM, Morrison RF. Skp2-mediated p27(Kip1) degradation during S/G2 phase progression of adipocyte hyperplasia. J Cell Physiol. 2007;211(1):101–111.
[35] Zhong S, Ji D-F, Li Y-G, et al. Activation of P27kip1-cyclin D1/E-CDK2 pathway by polysaccharide from phellinus linteus leads to S-phase arrest in HT-29 cells. Chem Biol Interact. 2013;206(2):222–229.
[36] Barr AR, Cooper S, Heldt FS, et al. DNA damage during S-phase mediates the proliferation-quiescence decision in the subsequent G1 via p21 expression. UK: Nat Commun. 2017; 8:14728.
[37] Huang B, Mu P, Chen X, et al. Aflatoxin B(1) induces S phase arrest by upregulating the expression of p21 via MYC, PLK1 and PLD1. Biochem Pharmacol. 2019;166:108–119.
[38] Beckerman R, Donner AJ, Mattia M, et al. A role for Chk1 in blocking transcriptional elongation of p21 RNA during the S-phase checkpoint. Genes Dev. 2009;23(11):1364–1377.
[39] Zhong S, Li YG, Ji DF, et al. Protocatechualdehyde induces S-phase arrest and apoptosis by stimulating the p27(KIP1)-cyclin A/D1-CDK2 and mitochondrial apoptotic pathways in HT-29 cells. Switzerland: Molecules; 2016; 21(7):934.
[40] Ravanko K, Järvinen K, Paasinen-Sohns A, et al. Loss of p27Kip1 from cyclin E/cyclin-dependent kinase (CDK) 2 but not from cyclin D1/CDK4 complexes in cells transformed by polyamine biosynthetic enzymes. Cancer Res. 2000;60(18):5244–5253.
[41] Ahn H, Im E, Lee DY, et al. Antitumor effect of pyrogallol via miR-134 mediated S phase arrest and inhibition of PI3K/AKT/Skp2/cMyc signaling in hepatocellular carcinoma. Int J Mol Sci. 2019;20(16):3985.